Light-particle-induced deexcitations of 3_1^- and 2_2^+ resonances of ^{12}C in extreme stellar conditions

A. Baishya ●,* S. Santra ●,† P. C. Rout, A. Pal, and T. Santhosh

Nuclear Physics Division, Bhabha Atomic Research Centre, Mumbai - 400085, India
and Homi Bhabha National Institute, Anushaktinagar, Mumbai - 400094, India

The particle-induced deexcitations of the 9.64 MeV, 3_1^- and 9.87 MeV, 2_2^+ resonances of ^{12}C increase the ^{12}C production rate in a very hot and dense stellar environment. The enhancements in ^{12}C production in such environments were estimated for a particle (n, p, and α) density of 10^6 g/cm^3 in the temperature range of $T_9 = 0.1$ to 10. Enhancement due to neutron-induced deexcitation was found to be the maximum. The net ^{12}C production rate due to the combined contributions from 7.65 (Hoyle state), 9.64, and 9.87 MeV states is much higher compared to the rate adopted by NACRE compilation. In case of a typical collapsing massive star with temperature dependent densities, for any of the 3_1^- or 2_2^+ resonances, the enhancement factor due to n, p, and α-induced deexcitations together can be as high as 600.

I. INTRODUCTION

All the elements present in our universe were created through a chain of nuclear reactions. Helium, the second most abundant element, was formed during the big bang nucleosynthesis via the fusion of protons and neutrons. However, consecutive fusion reactions halted at $A = 4$ due to the absence of stable nuclei at $A = 5$ and 8. Although ^{8}Be nuclei were produced in ^{4}He $+$ ^{4}He fusion, having a very short lifetime, they were rarely synthesized. In the 1950s, Hoyle and Salpeter [1,2] solved the first puzzle piece in understanding how heavy elements are created in stars. They addressed the bottleneck at $A = 5$ and 8, which was preventing the formation of heavier elements. Salpeter first proposed the sequential 3α reaction to produce ^{12}C to bypass the bottleneck. However, the nonresonant 3α reaction is not sufficient to explain the ^{12}C abundance in the universe. Hoyle proposed a resonant reaction to explain the observed abundance. This reaction is vital for creating carbon and oxygen in stars and for synthesizing heavier elements [3]. The 3α reaction proceeds through a series of resonant reactions. First, two ^{4}He combine to produce ^{8}Be in a resonant state, which then captures the third ^{4}He via a resonant capture reaction. At usual stellar temperatures, the 3α reaction is dominated by the resonant (Hoyle) state at 7.653 MeV. But, at higher temperatures ($T > 10^9 K$), the higher resonant states, i.e., 9.64 MeV (3_1^-) and 9.87 MeV (2_2^+) states, also contribute significantly [4].

The ^{12}C is produced in ground state when these resonant states decay by either γ emission or e^+-e^- pair production. In a third process, the resonance states of ^{12}C can deexcite while interacting with the surrounding particles. In particle-induced deexcitation (also known as up-scattering) process, a particle (neutron, proton, α, etc.) while getting scattered from an excited ^{12}C can take away the excitation energy from the excited ^{12}C and force it to come to the ground state or other lower excited states, as depicted in Fig. 1. These processes are known to be significant in certain stellar environments [5,6]. Recent studies [7,8] show how the 3α reaction rate is modified in high-density environments as a result of neutrons, protons and α-induced deexcitations of the Hoyle state.

The radiative width Γ_{rad} still determines ^{12}C production at the usual stellar regions. However, in cases where high temperatures and a high density of protons or neutrons are available, the enhancement due to particle-induced deexcitation from not only the Hoyle state but also the next higher resonance states becomes important.

The enhancements due to proton and neutron rich environments have been studied in [5–8], which show a significant enhancement in reaction rate where proton or neutron density reaches to $\approx 10^6$–10^7 g/cm^3 and temperature reaches to $T_9 = 10$ ($T_9 = 10^9$ K). Comparatively, the enhancement due to α-rich environments is much smaller [9]. However, all these studies other than the one by Truran [5] focused on the enhancement caused by particle-induced deexcitation only from the 7.65 MeV Hoyle state and enhancement due to higher resonances are ignored. The production of ^{12}C through the higher resonances, however, becomes comparable to that of the Hoyle state at higher temperatures ($T_9 > 5$). According to recent calculations by Tsumura *et al.* [10], when $T_9 > 5$, the stable ^{12}C production via either of the 9.64 and 9.87 MeV states becomes equal to or even higher than that through the Hoyle state. This is evident from Fig. 2, where the ratios of the radiative capture rate '$r_{3\alpha}^{E_x}$' to that of the Hoyle state '$r_{3\alpha}^{7.65}$' are compared, with E_x corresponding to resonance energies of 7.65, 9.64, and 9.87 MeV. These rates were calculated [11] following the procedure given in the supplemental material
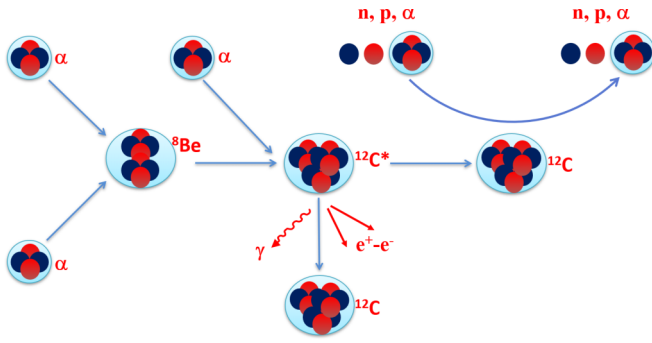

FIG. 1. A cartoon of the particle-induced deexcitation process, that competes with the spontaneous radiative deexcitation (γ or e^+-e^- pair emission).

of Ref. [10]. Using the radiative capture rates given by Fowler *et al.* [4], it was seen that the ^{12}C production via the 9.64 MeV state can be much larger (in fact ≈ 20 times at $T_9 \approx 100$) than that through the Hoyle state. In these temperature regions, it is therefore crucial to take into account the enhancement in 3α reaction rate due to particle-induced deexcitation from the the higher-lying 9.64 MeV and 9.87 MeV resonances.

In nucleosynthesis, the 3α reaction is vital because it bypasses the $A = 5$ and 8 bottleneck and opens the door to heavier elements. Production of s-process elements between ^{58}Fe and ^{96}Zr changes dramatically with changes in the 3α reaction rate [12]. Although the origins of p nuclei remain a topic of debate, the νp process during supernova explosions is a plausible explanation for their abundance, but it is not yet entirely understood. For an enhanced 3α reaction rate, the production of medium mass ($A = 60$–80) nuclei increases which act as proton poison and hence decreases the production of heavier mass ($A > 80$) [13] nuclei. Thus, the impact of increased 3α reaction rates in high-density environments is of profound interest.
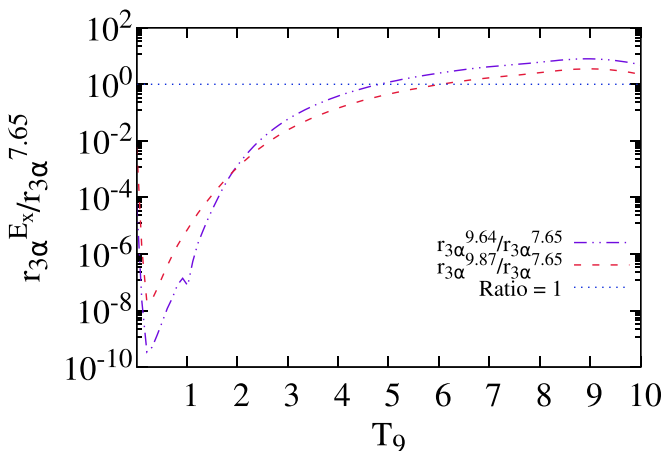

FIG. 2. Ratios of ^{12}C production each through the 9.64 and 9.87 MeV resonances to that through the 7.65 MeV Hoyle state. Here, $r_{3\alpha}^{E_x}$ denotes the radiative capture rates through different resonances at energies E_x.

In this work, we address the enhancement of the 3α reaction rate driven by deexcitation of ^{12}C from its 9.64 MeV, 3^- state and the 9.87 MeV, 2^+ state by inelastic scattering of neutron, proton, and α particles. We first describe the theoretical formalism for calculating the enhancement. Then, we discuss our results about the improvement of the 3α reaction rate and compare them with earlier results [5]. In the end, we aim to demonstrate how such enhancements affect stellar nucleosynthesis.

II. THEORETICAL FRAMEWORK

The expression for the enhancement in 3α reaction rate caused by particle-induced deexcitation was constructed using a theoretical formalism akin to that of Truran *et al.* [5] and Beard *et al.* [7]. However, the implementation of cross-sections for inelastic transitions of ^{12}C is similar to Beard *et al.* [7].

For particle-induced deexcitation, the average reaction rate, $\langle \sigma v \rangle_{x'x}$, for the transition from an excited state (with excitation energy, say, E_x) to the ground state or lower excited states, where x can be n, p, or α, is related to the lifetime $\tau_{x'x}$ of the transition as

$$\tau_{x'x}(^{12}C^{E_x}) = \frac{1}{N_x \langle \sigma v \rangle_{x'x}} \quad \text{sec}, \tag{1}$$

where E_x is 9.64 and 9.87 MeV in the present study and $\langle \sigma v \rangle_{x'x}$ can be obtained from its inverse reaction rate $\langle \sigma v \rangle_{xx'}$ by the principle of detailed balance given below:

$$\langle \sigma v \rangle_{x'x} = \left(\frac{2J+1}{2J'+1} \right) \exp(-Q/kT) \langle \sigma v \rangle_{xx'}. \tag{2}$$

Here, $\langle \sigma v \rangle_{xx'}$ is the average reaction rate for the transition from the ground state or lower excited states to the excited 9.64 or 9.87 MeV state. J and J' are the spins of initial and final states, and Q being the Q value of the reaction. Further, $\langle \sigma v \rangle_{xx'}$ can be expressed as

$$\langle \sigma v \rangle_{xx'} = \left(\frac{8}{\pi \mu} \right)^{1/2} \left(\frac{1}{kT} \right)^{3/2}$$
$$\times \int_0^\infty E' \sigma_{xx'}(E') \exp(-E'/kT) dE'. \tag{3}$$

The integral [Eq. (3)] gives the average reaction rate for the forward excitation and is over all possible relative energies following the Maxwellian distribution. This assumption is crucial and denotes the statistical behavior of the stellar environment.

Now, the enhancement in the production of ^{12}C in the ground state can be expressed as the ratio of production of ^{12}C via the particle-induced deexcitation process to production of ^{12}C via the radiative decay process. The production rate due to each process is related to its lifetime as, $r \propto \frac{1}{\tau}$. Thus, the enhancement can be expressed as

$$R_{xx} = r_{x'x}/r_\gamma = \tau_\gamma / \tau_{x'x} = \tau_\gamma N_x \langle \sigma v \rangle_{x'x}. \tag{4}$$

$R = 1$ indicates that the production of ^{12}C from either process is equal, whereas $R > 1$ indicates that the generation of ^{12}C via particle-induced deexcitation is greater.

Inserting $\tau_\gamma = 1.1 \times 10^{-14}$ sec, determined from the radiative widths [10] (almost equal for both the 9.64 MeV and the 9.87 MeV state), in Eq. (4) and expressing $\langle \sigma v \rangle_{x'x}$ using Eqs. (3) and (2), one can arrive at

$$R_{xx} = k_x \rho_x T_9^{-\frac{3}{2}} f_{\text{spin}} \int_0^\infty \sigma_{xx'}(E)(E + E_{th})$$
$$\times \exp(-11.605E/T_9)dE, \quad (5)$$

where E is the center of mass energy above the threshold energy for the reaction, E_{th}, ρ_x is the particle density in g/cm^3, $\sigma_{xx'}(E)$ is the cross section in mb, and f_{spin} is the spin factor ($\frac{2J+1}{2J'+1}$) and is equal to 1/7 for transitions from the ground state to the 3_1^- state and 1/5 for the transition from the ground state to the 2_2^+ state.

To calculate the enhancements due to the up-scattering of n, p, and α, the above equations have been applied independently by replacing the index x by n, p, and α, respectively. The values of k for the 9.64 MeV resonance used for each particle are $k_n = 4.220 \times 10^{-7}$, $k_p = 4.225 \times 10^{-7}$ and $k_\alpha = 5.922 \times 10^{-8}$, which were obtained by multiplying the k values for the particle-induced deexcitation from the Hoyle state [7] by a factor, $\tau_\gamma^{9.64}/\tau_\gamma^{7.65} = 0.06437$, as $k_x \propto \tau_\gamma$. Since, both the 9.64 and 9.87 MeV resonances have almost equal lifetime, the k values for the later are considered to be equal to those for the former, which are acceptable within the uncertainties of our calculation.

III. EVALUATION OF CROSS SECTIONS

As is evident from Eq. (5), $\sigma_{xx'}(E)$ values must be known to evaluate the integral. For excitation of ^{12}C to the 9.64 MeV state, experimental data on neutron-induced cross sections is scarce [15–17], and they also do not go all the way down to the essential energies just above the threshold. Although an experimental data set is available for the 9.64 MeV state in the energy range of our interest [14], the errors associated with the data points are very large, so it was not considered for the present calculations. Also, no cross section data are available for the 9.87 MeV state. In such cases, one can resort to the available theoretical techniques to determine the cross sections. One way to compute unmeasured cross sections is to use the Hauser-Feshbach (HF) statistical model [18,19], which has been considered for the present study employing the reaction code TALYS-1.96 [20].

The TALYS generated cross sections for inelastic excitations of ^{12}C from its ground state and 4.44 MeV state to the 9.64 and 9.87 MeV states are shown in Fig. 3. It may be noted that the default TALYS database does not contain the 9.87 MeV resonance and therefore the database was modified by hand in order to produce the cross sections for the g.s. → 9.87 and the 4.44 → 9.87 transitions. The transitions 7.65 → 9.64, 7.65 → 9.87, and 9.64 → 9.87 are not considered in the calculations as their contributions are negligible due to the reasons described later. For neutrons and protons, apart from the default optical model, three other optical models were used and for α, seven other models were used [20]. The uncertainty bands in Fig. 3 are thus due to different optical models. The experimental cross sections corresponding to the
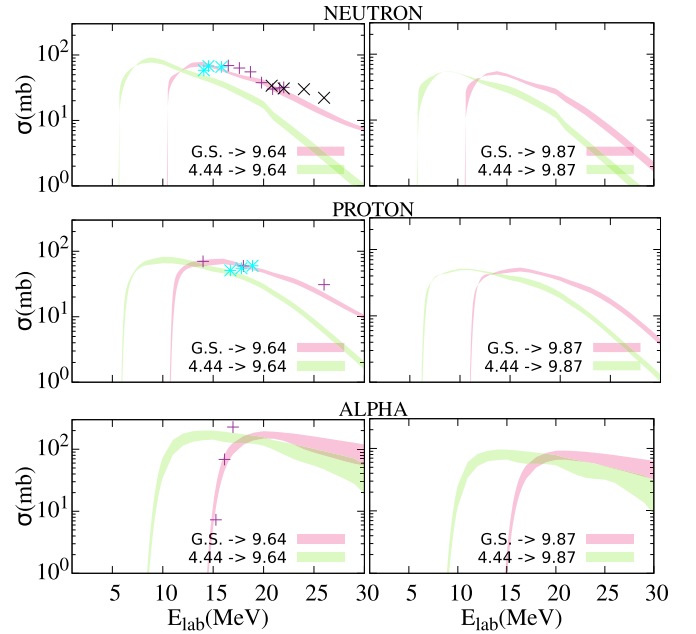

FIG. 3. Inelastic scattering cross sections for n (top panel), p (middle panel), and α (bottom panel). Available experimental cross sections for n [15–17], p [21,22], and for α [9] induced excitations of ^{12}C from its ground state to the 9.64 MeV state are shown by symbols.

inelastic excitation from the ground state to the 9.64 MeV state were also compared. It may be noted that the available experimental cross sections are for energies more than 2 MeV above the threshold energies and contribute significantly less to the integral of Eq. (5).

IV. RESULTS AND DISCUSSIONS

The ratio R_{nn} for the 9.64 MeV → g.s. transition was calculated first (i) using purely the TALYS generated cross section and then (ii) by combining the TALYS generated and experimental cross sections, similar to Ref. [7]. The difference between the two results was found to be very small ($<0.3\%$ even at an extreme temperature of $T_9 = 10$). This is because of the factor $\exp(-11.605E/T_9)$ inside the integrand in Eq. (5), which for small T_9 contributes only when E is very small, thus making the contributions from higher E negligible.

The TALYS cross sections were integrated up to 20 MeV above threshold using a subroutine that was already benchmarked [23]. The same results were obtained while integrating using the PYTHON-SciPy [24] package as well. Figure 4 depicts the calculated ratios (R_{nn}, R_{pp}, and $R_{\alpha\alpha}$) describing the enhancements in ^{12}C production due to particle-induced deexcitation from the 9.64 and 9.87 MeV resonances.

Figure 4 indicates that the increase in deexcitation caused by neutrons is greater than that caused by protons, which is in turn greater than that caused by α particles. This trend can be explained by considering the potential barriers present in each system. Neutrons only encounter a centrifugal barrier as they are charge-less and thus do not experience a Coulomb barrier. However, protons experience an additional Coulomb barrier
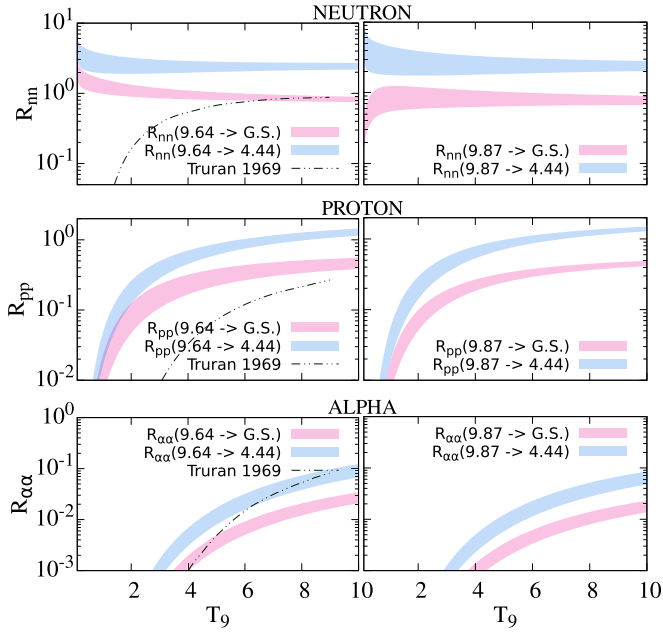
FIG. 4. Ratios (R_{nn} or R_{pp} or $R_{\alpha\alpha}$) of the particle-induced transition rates to the known radiative transition rates, calculated for a particle density of 10^6 g/cm^3. Enhancements calculated by Truran *et al.* [5] for the g.s. $\rightarrow$ 9.64 MeV transition, multiplied by 0.1 to match the particle density of 10^6 g/cm^3 considered for the present work, are also compared.

on top of their centrifugal barrier, and α particles experience an even higher Coulomb barrier.

The ratios (R_{nn}, R_{pp}, or $R_{\alpha\alpha}$) for the 9.64(9.87) $\rightarrow$ 4.44 MeV transitions are larger than the 9.64(9.87) $\rightarrow$ g.s. transitions. This is mainly due to the factor f_{spin}, which for the 9.64(9.87) $\rightarrow$ 4.44 MeV transition is five times larger than the 9.64(9.87) $\rightarrow$ g.s transition. The total enhancement for deexcitation of the 9.64(9.87) MeV state resulting from three possible transitions can be calculated as follows:

$$R_{xx}(\text{total}) = R_{xx}(9.64 \rightarrow \text{g.s.}) + R_{xx}(9.64 \rightarrow 4.44)$$
$$+ \frac{\Gamma_{xx}^{7.65}(\text{total})}{\Gamma^{7.65}} \times R_{xx}(9.64 \rightarrow 7.65), \quad (6)$$

where

$$\Gamma_{xx}^{7.65}(\text{total}) = \Gamma_{\gamma}^{7.65} \times (R_{xx}(7.65 \rightarrow \text{g.s.})$$
$$+ R_{xx}(7.65 \rightarrow 4.44)). \quad (7)$$

Given that $\frac{\Gamma_{\gamma}^{7.65}}{\Gamma^{7.65}} = 4.03 \times 10^{-4}$ [25], the third term in Eq. (6) can be neglected. For the same reason, the 9.64 $\rightarrow$ 7.65 transition was not considered any further. For the 9.87 MeV state there will be a fourth term in Eq. (6) equal to $\frac{\Gamma_{xx}^{9.64}(\text{total})}{\Gamma^{9.64}} \times R_{xx}(9.87 \rightarrow 9.64)$ which is again negligible and is ignored for total enhancement calculation.

One noteworthy observation is that the calculated R_{nn} shows a decreasing trend similar to that of Beard *et al.* [7] but differs from that of Truran *et al.* [5] (see dash-dot-dotted line in Fig. 4). However, for proton and α, the R_{pp} and $R_{\alpha\alpha}$

values follow an increasing trend similar to both Beard and Truran.

It is apparent that the calculated ratios R_{nn} and R_{pp} are greater than those predicted in the previous work [5]. This discrepancy is due to the use of different cross sections ($\sigma_{nn'}$, $\sigma_{pp'}$, $\sigma_{\alpha\alpha'}$), τ_γ and energy range of integration. Truran *et al.* [5] employed a constant cross-section method instead of the energy-dependent cross section used in the present work. Also, they performed integration only up to 0.5 MeV above the threshold, whereas the range of the present integration is up to 20 MeV. The present study does not include enhancements due to electromagnetic effects, which are insignificant for $\rho \ll 10^9$ g/cm^3 [26]. The enhancement in deexcitation of the 9.87 MeV state is presented and is similar to the values found for the 9.64 MeV state. This is because the cross sections as well as the radiative decay widths for both of these states are nearly the same.

To realize how the enhancements affect the total 3α reaction rate and thus the ^{12}C production, the enhanced partial 3α reaction rates through individual resonances above the breakup threshold of 7.27 MeV need to be calculated. Coughlan and Fowler [27] only considered the 7.65 MeV resonant state to calculate the 3α reaction rate; however, three resonance states (7.65 MeV Hoyle state, an assumed 2^+ resonance at 9.2 MeV, and the 9.64 MeV state) are considered for the calculation by Angulo *et al.* [28] for the NACRE compilation. Tsumura *et al.* [10] found a much higher experimental value of Γ_γ (61 meV compared to 2 meV considered by Angulo [28]) for the 9.64 MeV state, which results in a larger contribution from this state, but due to a poor assumption of the 2^+ resonance at 9.2 MeV (not found to this date), the 3α rate at higher temperatures is higher in NACRE. In the present work, the total enhanced 3α reaction rate for density of 10^6 g/cm^3 was calculated by multiplying the individual 3α radiative capture rates of 7.65, 9.64, and 9.87 MeV resonances (which were used to obtain Fig. 2) by '$1 + R_{nn}$', where R_{nn} is the respective enhancement factor due to neutron-induced deexcitation. The ratios of the enhanced 3α rates to the pure capture rate adopted in NACRE are shown in Fig. 5. The total radiative capture rate obtained by Tsumura *et al.* [10] is compared and shown as a blue dash-dot-dotted line. Also compared are the results by Garrido and Jensen [29] (green long dashed line). They used the four-body direct and sequential recombination model and considered the 9.2 MeV 2^+ resonance along with the 7.65 MeV and 9.64 MeV resonances, same as considered by Angulo [28] for NACRE compilation. A much higher 3α rate can be seen due to neutron-induced enhancement at lower T_9 (black solid line in Fig. 5). A large 3α reaction rate at lower temperatures will have a profound effect on helium-burning medium-mass stars, which can produce huge amounts of ^{12}C in the presence of a neutron-rich environment. Whereas, in very hot and dense mediums (like supernovae cores, neutron stars, etc.), all three particles (neutron, proton, and α) induced enhanced 3α reaction rate, will increase the ^{12}C production.

Finally, we studied the implications of the large enhancement factors obtained in the present study in a model collapsing star. For such a star of mass 1.5 times the solar mass, the Cowling model can be applied [1], where the density changes as a function of temperature, $\rho \propto 10^6 T_9^3$. Thus, when
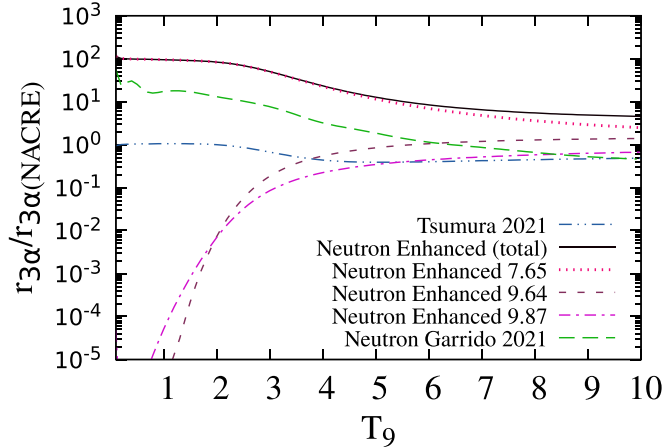
FIG. 5. Ratio of 3α reaction rate (neutron-induced deexcitation + radiative capture) due to individual resonances (7.65, 9.64, and 9.87 MeV) above the threshold as well as the sum total rate (black solid line) due to all these three resonances to the radiative capture rate adopted from the NACRE compilation. The 3α reaction rate (i) considering improved radiative capture calculated by Tsumura [10] (blue dash-dot-dotted line) and (ii) considering four-body direct and sequential recombination by Garrido and Jensen [29] (green long dashed line) are also shown.

a star is compressed, its temperature increases accordingly. The model fairly represents the density up to $T_9 = 5$. Our results indicate that much higher enhancements in the 3α reaction rate are expected in such scenarios compared to the constant density assumption used so far in our previous calculations. The enhancement in such case due to each of the two states (9.64 MeV and 9.87 MeV) is illustrated in Fig. 6, which clearly shows a significant increase in the total enhancement factors with $R_{nn} = 450$–500 and $R_{pp} = 110$–125.

In the quest for the enhancement in ^{12}C production, similar calculations were extended for several astrophysical sites, such as, the sun, white dwarf stars, red giant stars, AGB stars,
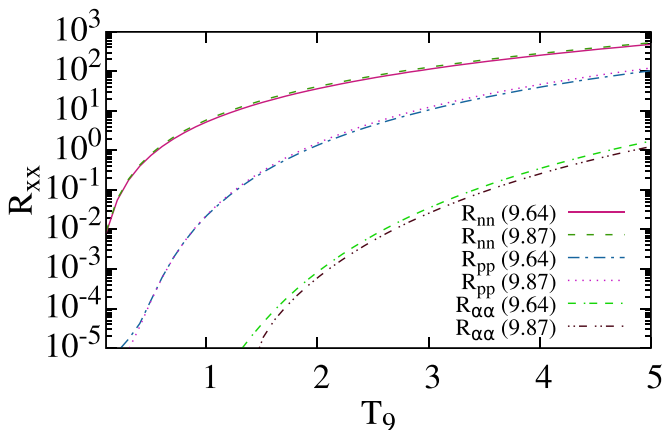

FIG. 6. Enhancements in 3α reaction rate using the Cowling model of a collapsing star (using the default TALYS parameters), where the density varies as a function of temperature, $\rho \propto 10^6 T_9^3$. Enhancement due to both the 9.64 MeV and the 9.87 MeV states shown.

neutron stars, supernovae, and x-ray bursts, which have a wide range of densities (10^2–10^{18} g/cm^3) and temperatures (0.01–100 GK). The neutron-induced enhancements for these cases were calculated and found to be very large in the hot and dense regions like white dwarfs, AGB stars, supernovae, neutron stars, and x-ray bursts, but negligible for the cases of the sun and red giant stars. It may be noted that the inclusion of corrections due to the electromagnetic effects [26] will lead to further enhancements in all these cases.

V. SUMMARY AND CONCLUSIONS

We performed a comprehensive study of light particles like neutron-, proton-, and α-induced deexcitations of the 9.64 MeV, 3_1^- state and 9.87 MeV, 2_2^+ state of ^{12}C that enhance the ^{12}C production rate in extreme stellar environments. The enhancements in ^{12}C production in such environments were estimated for a particle (n, p, and α) density of 10^6 g/cm^3 in the temperature range of $T_9 = 0.1$ to 10. The estimated enhancements for the 9.64 MeV state due to neutrons and protons were found to be larger than those of Truran *et al.* [5], the only other available calculation for the 9.64 MeV state, whereas enhancements for the 9.87 MeV state are presented. For both the states, the enhancement due to neutron-induced deexcitation was found to be the maximum. The net ^{12}C production rate due to the combined contribution from the 7.65, 9.64, and 9.87 MeV states is much higher compared to the rate adopted by NACRE compilation. The present formalism was employed in the case of a typical collapsing massive star with temperature-dependent densities, and the combined enhancement factor for each of the two states was estimated to be about 600. Similar calculations were extended to different astrophysical sites. The neutron-induced (the most dominant) enhancements for these cases were found to be very large in cases of hot and dense regions like white dwarfs, AGB stars, supernovae, neutron stars, and x-ray bursts, but negligible for the sun-like stars and red giant stars.

In principle, these types of calculations can be extended to other reactions where the particle decay width is much larger compared to the radiative decay width, making the reaction rate proportional to the radiative decay width and, thus, sensitive to enhancements by inelastic reactions. Accurate experimental cross sections near the threshold will surely improve upon our findings. Experimentally, proton and α-induced inelastic cross sections for the ground state to the 9.64 MeV state can be measured fairly easily, but measuring the neutron-induced cross sections can be tricky and needs to be attempted with careful consideration. For neutrons, the uncertainty regarding the beam energy, beam flux monitoring plays a crucial role along with an efficient detection mechanism. However, intermediate transitions like from the 4.44 MeV to 9.64 MeV state or 9.87 MeV state cannot be measured directly. They can be addressed, however, using R-matrix techniques [8], but detailed knowledge of all resonances lying close to the threshold is required. Developing a robust R-matrix formalism for such problems will definitely be a worthwhile exercise.

[1] F. Hoyle, Astrophys. J. Suppl. Series **1**, 121 (1955).

[2] E. E. Salpeter, Astrophys. J. **115**, 326 (1952).

[3] C. West, A. Heger, and S. M. Austin, Astrophys. J. **769**, 2 (2013).

[4] W. A. Fowler, G. R. Caughlan, and B. A. Zimmerman, Annu. Rev. Astron. Astrophys. **5**, 525 (1967).

[5] J. W. Truran and B. Z. Kozlovsky, Astrophys. J. **158**, 1021 (1969).

[6] C. N. Davids and T. I. Bonner, Astrophys. J. **166**, 405 (1971).

[7] M. Beard, S. M. Austin, and R. Cyburt, Phys. Rev. Lett. **119**, 112701 (2017).

[8] J. Bishop, C. E. Parker, G. V. Rogachev *et al.*, Nat. Commun. **13**, 2151 (2022).

[9] J. F. Morgan and D. C. Weisser, Nucl. Phys. A **151**, 561 (1970).

[10] M. Tsumura, T. Kawabata, Y. Takahashi *et al.*, Phys. Lett. B **817**, 136283 (2021).

[11] T. Kawabata (private communication).

[12] C. Tur, A. Heger, and S. M. Austin, Astrophys. J. **702**, 1068 (2009).

[13] S. Wanajo, H. T. Janka, and S. Kubono, Astrophys. J. **729**, 46 (2011).

[14] B. Antolković, I. Šlaus, D. Plenković, P. Macq, and J. P. Meulders, Nuclear Phys. A **394**, 87 (1983).

[15] N. Olsson, B. Trostell, and E. Ramstrom, Phys. Med. Biol. **34**, 909 (1989).

[16] A. S. Meigooni, R. W. Finlay, J. S. Petler, and J. P. Delaroche, Nucl. Phys. A **445**, 304 (1985).

[17] D. Schmidt and B. R. L. Siebert, Nucl. Instrum. Methods Phys. Res. A **342**, 544 (1994).

[18] W. Hauser and H. Feshbach, Phys. Rev. **87**, 366 (1952).

[19] L. Wolfenstein, Phys. Rev. **82**, 690 (1951).

[20] A. J. Koning, S. Hilaire, and M. C. Duijvestijn, *International Conference on Nuclear Data for Science and Technology* (2007), pp. 211–214, https://doi.org/10.1051/ndata:07767.

[21] M. Harada *et al.*, J. Nucl. Sci. Technol. **36**, 313 (1999).

[22] R. W. Peelle, Phys. Rev. **105**, 1311 (1957).

[23] A. Baishya, S. Santra, A. Pal, and P. C. Rout, Phys. Rev. C **104**, 024601 (2021).

[24] P. Virtanen, R. Gommers, and T. E. Oliphant, Nature Methods **17**, 261 (2020).

[25] M. Freer and H. O. U. Fynbo, Prog. Part. Nucl. Phys. **78**, 1 (2014).

[26] P. B. Shaw and D. D. Clayton, Phys. Rev. **160**, 1193 (1967).

[27] G. R. Caughlan and W. A. Fowler, At. Data Nucl. Data Tables **40**, 283 (1988).

[28] C. Angulo, M. Arnould, M. Rayet *et al.*, Nucl. Phys. A **656**, 3 (1999).

[29] E. Garrido and A. S. Jensen, Phys. Rev. C **103**, 055813 (2021).